Supplementary Information

Supplementary Video S1: Wing skeletal motion is non-planar and deviates from the anatomical plane. In the ventral view, the wing bones appear to follow a traditional four-bar 'drawing parallels' pattern. However, when we rotate to the anterior view, we see the wing bones move out of plane, demonstrating that the overall motion is non-planar and therefore a 2D 'drawing parallels' model is insufficient. Skeletal motion is shown in the reference frames shown in figure 2.

Supplementary Video S2: Including wrist bones in a six-bar mechanism improves the model's performance in tracking measured wing bone motion. This video compares the four-bar wing model with fused wrist bones and a full six-bar wing model with the measured bone locations (both mechanisms are shown as cartoons in Figure 6). The measured locations of the large bones are shown in grey, while the modeled bones are shown in color.

Table S1 (Weights and sexes of the pigeon cadavers in the experiment.): Weights and sexes of the pigeon cadavers in the experiment.

ID	Sex	Weight
1	M	456.5 g
2	F	447.4 g
3	F	397.9 g

Table S2 (Marker cluster sizes): Nominal marker cluster sizes have been designed to be unique for ease of identification using Monte Carlo simulation.

Cluster	Leg 1 length (mm)	Leg 2 length (mm)	Leg 3 length (mm)
1 (keel)	11	13	19
2 (humerus)	15	18	22
3 (radius)	14	16	25
4 (ulna)	12	21	23
5 (carpometacarpus)	17	20	24

Table S3 (List of mechanisms tested): Permutations of four, five and six-bar mechanisms covering different models of joint types and wrist bones. The ID numbers here correspond to each mechanism model evaluated in Figure S4, which shows the error each mechanism had in approximating the measured motion for every pigeon and cycle. The next two columns show the number of mechanism bars and degrees of freedom of that mechanism (DOF). 'Yes' and 'no' in the 'Radiale?' and 'Ulnare?' columns denote whether the bone is included in the model with a pin joint to the radius and/or a sliding joint to the ulna respectively, increasing a basic four-bar mechanism to a five or six-bar one. The remaining columns denote joint types of the remaining joints. 'Spherical' refers to a joint with three rotational degrees of freedom and all translational degrees of freedom locked, and 'pin' refers to a joint with only one rotational degree of freedom.

Radius-humerus' refers to the joint connecting the distal end of the humerus to the proximal end of the humerus. 'Ulna-humerus' refers to the joint connecting the distal end of the humerus to the proximal end of the ulna. 'Carpo-radius' refers to the joint connecting the distal end of either the radius-radiale hybrid (if the radiale is not included) or the radiale to the proximal end of the carpometacarpus. 'Carpo-ulna' refers to the joint connecting the distal end of either the ulna-ulnare hybrid (if the ulnare is not included) or the ulnare to the proximal end of the carpometacarpus.

ID	Number of bars	DOF	Radiale?	Ulnare?	Radius-humerus	Ulna-humerus	Carpo-radius	Carpo-ulna
1	4	0	no	no	spherical	pin	pin	pin
2	5	1	no	yes	pin	pin	pin	spherical
3	5	1	yes	no	spherical	pin	pin	pin
4	5	1	no	yes	pin	pin	spherical	pin
5	4	2	no	no	pin	spherical	pin	spherical
6	5	1	yes	no	pin	spherical	pin	pin
7	5	1	yes	no	pin	pin	spherical	pin
8	5	1	no	yes	spherical	pin	pin	pin
9	5	1	yes	no	pin	pin	pin	spherical
10	4	2	no	no	pin	pin	spherical	spherical
11	5	1	no	yes	pin	spherical	pin	pin
12	4	2	no	no	spherical	pin	spherical	pin
13	4	2	no	no	spherical	pin	pin	spherical
14	4	2	no	no	pin	spherical	spherical	pin
15	4	2	no	no	spherical	pin	pin	spherical
16	5	3	no	yes	pin	pin	spherical	spherical
17	5	1	no	yes	pin	pin	pin	spherical
18	5	1	no	yes	spherical	pin	pin	pin
19	5	1	no	yes	pin	pin	spherical	pin
20	5	1	no	yes	pin	spherical	pin	pin
21	5	3	yes	no	pin	spherical	pin	spherical
22	4	2	no	no	spherical	spherical	pin	pin
23	4	2	no	no	pin	spherical	pin	spherical
24	5	3	yes	no	spherical	pin	spherical	pin
25	6	2	yes	yes	spherical	pin	pin	pin
26	5	3	yes	no	spherical	pin	pin	spherical
27	4	2	no	no	spherical	pin	spherical	pin
28	4	2	no	no	spherical	spherical	pin	pin
29	5	3	yes	no	spherical	spherical	pin	pin
30	6	2	yes	yes	pin	spherical	pin	pin
31	5	3	no	yes	spherical	spherical	pin	pin
32	5	3	yes	no	pin	spherical	spherical	pin
33	6	2	yes	yes	pin	pin	pin	spherical
34	4	4	no	no	spherical	spherical	pin	spherical

35	4	2	no	no	pin	spherical	spherical	pin
36	6	2	yes	yes	pin	pin	spherical	pin
37	5	3	no	yes	pin	spherical	pin	spherical
38	6	4	yes	yes	spherical	spherical	pin	pin
39	4	4	no	no	spherical	spherical	spherical	pin
40	5	3	no	yes	spherical	pin	spherical	pin
41	4	4	no	no	spherical	spherical	pin	spherical
42	4	4	no	no	spherical	spherical	spherical	pin
43	6	4	yes	yes	spherical	pin	spherical	pin
44	5	3	no	yes	spherical	spherical	pin	pin
45	4	2	no	no	pin	pin	spherical	spherical
46	5	3	no	yes	spherical	pin	pin	spherical
47	5	5	yes	no	spherical	spherical	pin	spherical
48	5	3	no	yes	spherical	pin	spherical	pin
49	5	3	yes	no	pin	pin	spherical	spherical
50	5	5	yes	no	spherical	spherical	spherical	pin
51	5	3	no	yes	pin	spherical	spherical	pin
52	5	3	no	yes	pin	spherical	pin	spherical
53	5	3	no	yes	pin	pin	spherical	spherical
54	4	4	no	no	spherical	pin	spherical	spherical
55	6	4	yes	yes	pin	spherical	spherical	pin
56	6	4	yes	yes	spherical	pin	pin	spherical
57	5	3	no	yes	spherical	pin	pin	spherical
58	4	4	no	no	pin	spherical	spherical	spherical
59	5	5	no	yes	spherical	spherical	spherical	pin
60	5	5	yes	no	spherical	pin	spherical	spherical
61	5	3	no	yes	pin	spherical	spherical	pin
62	6	4	yes	yes	pin	spherical	pin	spherical
63	5	5	no	yes	spherical	spherical	pin	spherical
64	6	6	yes	yes	spherical	spherical	spherical	pin
65	4	4	no	no	pin	spherical	spherical	spherical
66	4	4	no	no	spherical	pin	spherical	spherical
67	6	4	yes	yes	pin	pin	spherical	spherical
68	5	5	no	yes	spherical	pin	spherical	spherical
69	4	6	no	no	spherical	spherical	spherical	spherical
70	5	5	no	yes	spherical	pin	spherical	spherical
71	5	5	yes	no	pin	spherical	spherical	spherical
72	5	5	no	yes	pin	spherical	spherical	spherical
73	6	6	yes	yes	spherical	pin	spherical	spherical
74	6	6	yes	yes	spherical	spherical	pin	spherical
75	5	5	no	yes	pin	spherical	spherical	spherical
76	5	5	no	yes	spherical	spherical	spherical	pin
77	5	7	yes	no	spherical	spherical	spherical	spherical

78	6	6	yes	yes	pin	spherical	spherical	spherical
79	5	5	no	yes	spherical	spherical	pin	spherical
80	4	6	no	no	spherical	spherical	spherical	spherical
81	5	7	no	yes	spherical	spherical	spherical	spherical
82	6	8	yes	yes	spherical	spherical	spherical	spherical
83	5	7	no	yes	spherical	spherical	spherical	spherical

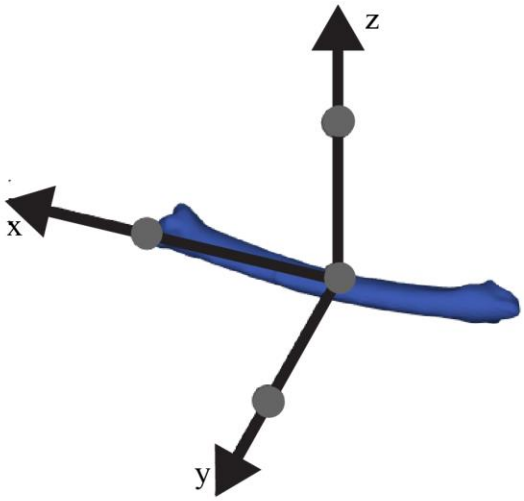

Figure S1 (Standardized bone marker placements): Standardized bone marker placements, shown for the ulna. We define the bone axes to be a right-handed coordinate system comprising the principle axes of each bone, with the x-axis corresponding to the minimal principle axis pointing distally. We place the origin at the center of mass and place the computational marker points 30 mm out along the x, y and z-axes for center and axis of rotation calculations.

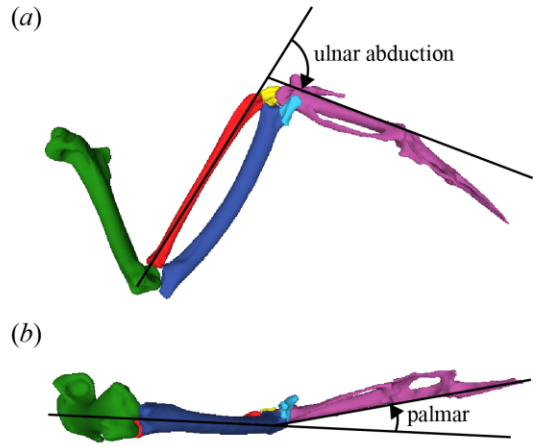

Figure S2 (Wrist angle definitions): Pigeon wrist angles defined for Figure 3. They enable comparison of bird and human wrist abduction/adduction and palmar/dorsal motion. (*a*) Ulnar abduction and radial adduction refer to rotation of the carpometacarpus in the wing plane. This is defined as the angle between the carpometacarpus and the radius when projected into the humerus-radius plane. (*b*) Palmar and dorsal refer to out of plane motion. This is defined as the angle between the carpometacarpus and the anatomical (humerus-radius) plane.

Derivation of the effect of a slider joint on the center of rotation:

The ulna-carpometacarpus center of rotation offset (Figure 8) can be explained by the hybrid joint function of the ulnare: The ulnare slides along the ulna and the carpometacarpus rotates around the ulnare. We show mathematically how this combined motion of the ulnare shifts the center of rotation if we assume a single joint represents the ulnare as in the four-bar paradigm. Consider a body that rotates by θ and translates by d between two positions. Use two points that are each length l away from the line that would go through the center if there were no translations at the radial position r (although any two points could be used). These points are P_1 and P_2 (Figure 8), and have the positions as follows:

$$P_1 = \begin{bmatrix} \frac{d}{2} + r\sin\left(\frac{\theta}{2}\right) - l\cos\left(\frac{\theta}{2}\right) \\ -r\cos\left(\frac{\theta}{2}\right) - l\sin\left(\frac{\theta}{2}\right) \end{bmatrix}$$

$$P_2 = \begin{bmatrix} \frac{d}{2} + r\sin\left(\frac{\theta}{2}\right) + l\cos\left(\frac{\theta}{2}\right) \\ -r\cos\left(\frac{\theta}{2}\right) + l\sin\left(\frac{\theta}{2}\right) \end{bmatrix}$$

After the translation and rotation they are in new positions P_1' and P_2':

$$P_1' = \begin{bmatrix} -\frac{d}{2} - r\sin\left(\frac{\theta}{2}\right) - l\cos\left(\frac{\theta}{2}\right) \\ -r\cos\left(\frac{\theta}{2}\right) + l\sin\left(\frac{\theta}{2}\right) \end{bmatrix}$$

$$P_2' = \begin{bmatrix} -\frac{d}{2} - r\sin\left(\frac{\theta}{2}\right) + l\cos\left(\frac{\theta}{2}\right) \\ -r\cos\left(\frac{\theta}{2}\right) - l\sin\left(\frac{\theta}{2}\right) \end{bmatrix}$$

The center of rotation will be the intersection of the perpendicular bisectors of $\overline{P_1P_1'}$ and $\overline{P_2P_2'}$. The midpoints are:

$$M_1 = \frac{1}{2}(P_1 + P_1') = \begin{bmatrix} -l\cos\left(\frac{\theta}{2}\right) \\ -r\cos\left(\frac{\theta}{2}\right) \end{bmatrix}$$

$$M_2 = \frac{1}{2}(P_2 + P_2') = \begin{bmatrix} l\cos\left(\frac{\theta}{2}\right) \\ -r\cos\left(\frac{\theta}{2}\right) \end{bmatrix}$$

The slopes of $\overline{P_1P_1'}$ and $\overline{P_2P_2'}$ are:

$$m_1 = \frac{-2l\sin\left(\frac{\theta}{2}\right)}{d + 2r\sin\left(\frac{\theta}{2}\right)}$$

$$m_2 = \frac{2l\sin\left(\frac{\theta}{2}\right)}{d + 2r\sin\left(\frac{\theta}{2}\right)}$$

And so the two lines which intersect at the average center of rotation are:

$$y + r\cos\left(\frac{\theta}{2}\right) = \frac{d + 2r\sin\left(\frac{\theta}{2}\right)}{2l\sin\left(\frac{\theta}{2}\right)}\left(x + l\cos\left(\frac{\theta}{2}\right)\right)$$

$$y + r\cos\left(\frac{\theta}{2}\right) = -\frac{d + 2r\sin\left(\frac{\theta}{2}\right)}{2l\sin\left(\frac{\theta}{2}\right)}\left(x - l\cos\left(\frac{\theta}{2}\right)\right)$$

These lines intersect at the point $\left[0, \frac{d}{2\tan\frac{\theta}{2}}\right]$, which is the center of rotation. A pure rotation would have a center of rotation at $[0,0]$, so this point is shifted away from the pure rotation by $\frac{d}{2\tan\theta}$. This shift is directly proportional to the distance, d, that the body slides, which is inversely related to the angle the wrist rotates, θ.

Table S4 (Joint locations): Locations of joints in the six-bar model shown in the main text. Locations are given in the coordinate system of each bone where the origin is the bone's center of mass, x is oriented along the long axis, and y and z are the other two principle axes in a right-handed coordinate system as shown in Figure S1. The joint axis orientations for the pin and slider joints are given as unit vectors in this coordinate system.

Joint (Type)	In which bone	Location in bone (mm)	Axis Orientation
Humerus-radius (spherical joint)	Humerus	$(23.5, 4.1, -1.0)^T$	N/A
	Radius	$(-25.6, -0.2, -2.4))^T$	N/A
Radius-radiale (pin joint)	Radius	$(28.9, 2.3, -1.3)^T$	$(0.42, 0.90, 0.14)^T$
	Radiale	$(9.6, 6.9, 9.1)^T$	$(0.45, 0.37, 0.81)^T$
Radiale-carpometacarpus (spherical joint)	Radiale	$(-4.2, -4.1, 2.9)^T$	N/A
	Carpometacarpus	$(-26.4, -2.2, 0.9)^T$	N/A
Ulnare-carpometacarpus (spherical joint)	Carpometacarpus	$(-24.4, -1.8, -1.0)^T$	N/A
	Ulnare	$(3.8, 2.5, 0.2)^T$	N/A
Ulna-ulnare (slider joint)	Ulna	$(26.3, -0.7, -1.0)^T$	$(0.98, 0.14, -0.02)^T$
	Ulnare	$(-9.1, -1.0, 1.7)^T$	$(-0.86, 0.51, 0.07)^T$
Humerus-ulna (spherical joint)	Humerus	$(26.4, -3.9, -1.5)^T$	N/A
	Ulna	$(-26.9, -3.2, 5.0)^T$	N/A

Table S5 (6 bar mechanism link lengths): Link lengths for a three dimensional four-bar mechanism with four links that best approximate the measured data. Standard deviations are across the three pigeons.

Bone	**Effective bar length (mm)**
Humerus	7.1 ±3.6
Radius	53.9 ± 1.5
Ulna	57.4 ± 2.9
Carpometacarpus	9.9 ± 5

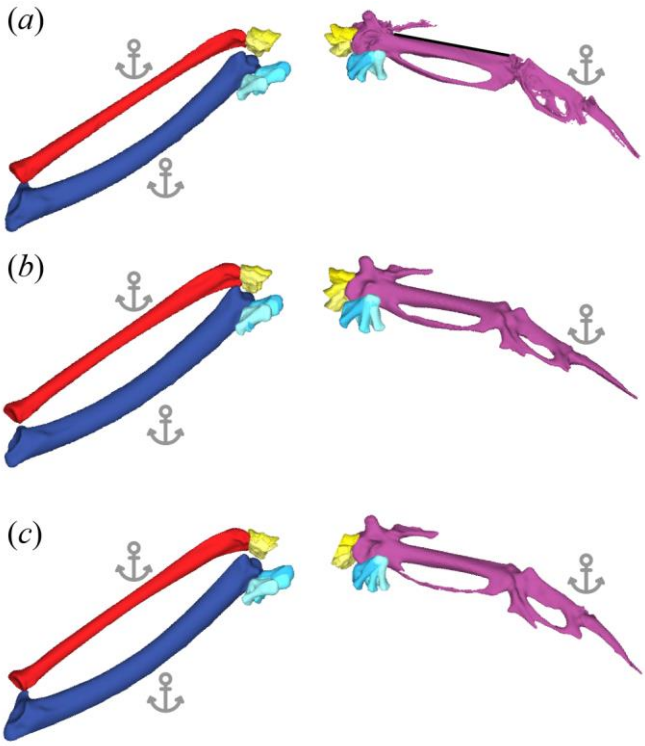

Figure S3 (Wrist bone motion for all three pigeons): Radiale and ulnare motion about the carpometacarpus, radius, and ulna for each of the three pigeon cadavers (A, B, C) based on CT-scan data (shown in the two extreme positions and one intermediate position).

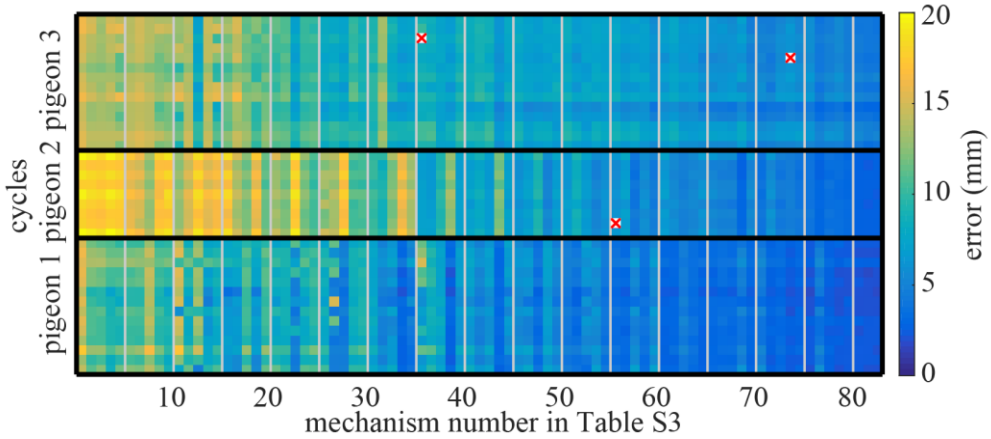

Figure S4 (All simulation results): Results by pigeon and cycle for each simulation listed in Table S3. The color map indicates the error level determined by the least-squares error minimization algorithm, blue indicates a cycle and mechanism combination that fits the data well. A red ‘x’ indicates that the algorithm was unable to converge for this particular cycle.